DOI: 10.1002/chem.200901213

Insight into the Complexation Mode of Bis(nitrilotriacetic acid) (NTA) Ligands with Ni^{2+} Involved in the Labeling of Histidine-Tagged Proteins

Marie Brellier,*[a, c] Bernard Barlaam,[b] Charles Mioskowski,[a] and Rachid Baati*[a]

In memory of Dr. Charles Mioskowski

Abstract: According to literature reports and our own findings, the binding of new Ni^{2+}-preloaded bis(nitrilotriacetic acid) (NTA) ligands with polyhistidine-tagged proteins has been found to be accompanied by a one- to two-order-of-magnitude increase in affinity, compared to the binding of a single Ni^{2+}-preloaded NTA moiety. In spite of the introduction of a second NTA chelating group, a cooperative effect that is less than the theoretical maximum has been observed. Herein, we present a rational explanation for the observed stability of the ternary complex involving the postulated bis-NTA–$(Ni^{2+})_2$ species and multivalent polyhistidine tags. We have found that prior to the formation of the ternary complex, the Ni^{2+}-preloading step of bis-NTA ligands does not form the expected bis-NTA–$(Ni^{2+})_2$ exclusively. Instead of the major formation of bis-NTA–$(Ni^{2+})_2$ species, it appears that cyclic discrete 1:1 and 2:2 entities are predominantly formed. It is proposed that these species interact upon ring-opening with multivalent histidine tags. The occurrence of this phenomena accounts for the overall one- to two-order-of-magnitude increase in affinity of ternary complexes involving bis-NTA ligands.

Keywords: chelates · fluorescent probes · microcalorimetry · proteins · ternary complexes

Introduction

Proteomics, the analysis of the entire set of proteins of a biological system, is a challenging area of research that has emerged in recent decades, and is one that requires new tools for handling, labeling, and modifying proteins. Many techniques have been developed to site-selectively incorporate molecular probes into proteins present in living cells or ex vivo.[1–12] The most promising results have emerged from two techniques using small and easily handled organic fluorescent probes that can be attached to proteins at specific sites. The strategy of Tsien and co-workers is based on the labeling of genetically altered proteins by small biarsenic fluorophores,[1] and the second technique exploits the ability of Ni^{2+}, chelated by nitrilotriacetic acid (NTA), to anchor histidine residues. The binding phenomenon has been extensively employed for the single-step purification,[13] detection,[14,15] and isolation of proteins and enzymes modified at the N or C terminus with a series of histidine residues. This well-documented technique has also been applied to the immobilization of proteins on surfaces and for tethering to membranes.[16,17] However, although stable and strong binding has been observed between polyhistidine-tagged protein and surfaces densely covered with NTA–Ni^{2+} ($K_D \approx 10^{-13}$ M),[16a,18] the binding affinity of a single NTA–Ni^{2+} chelator with oligohistidine remains weak ($K_D \geq 10^{-6}$ M).[19–21] This dramatic decrease of the affinity constant has been ascribed to the multivalent interactions offered to multiple mono-NTA binders with polyhistidine tags.[22] Therefore, the design and synthesis of supramolecules bearing several NTA moieties appeared to be a rational strategy for the development of probes displaying a strong affinity for histidine-tagged proteins. This strategy, which uses bis-NTA ligands was first introduced and validated by Tampé et al.,[19] and was recently illustrated by Ebright, Piehler, and Tampé for

[a] Dr. M. Brellier, Dr. C. Mioskowski, Dr. R. Baati
Université de Strasbourg, Faculté de Pharmacie CNRS/UMR 7199
74, route du Rhin, 67401 Illkirch (France)
Fax: (+33) 368-854-306
E-mail: baati@bioorga.u-strasbg.fr

[b] Dr. B. Barlaam
Astra-Zeneca, Chemin Vrilly, 51100 Reims (France)

[c] Dr. M. Brellier
Present address: NovAliX, Blvd S. Brant
BP30170, 67405 Illkirch (France)
E-mail: mb@novalix-pharma.com

Supporting information for this article is available on the WWW under http://dx.doi.org/10.1002/chem.200901213.

the complexation of Ni^{2+}-preloaded bis-, tris-, and tetra-NTA with polyhistidine tags, respectively.[20,23,24] These multivalent probes exhibited lower dissociation constants compared to the one observed with Ni^{2+}-preloaded mono-NTA ligands for the complexation with H_6-tagged proteins: K'_D(mono-NTA) ≈ 10–14 μM; K'_D(bis-NTA) ≈ 0.27–2 μM; K'_D(tris-NTA) ≈ 23 nM and K'_D(tetra-NTA) ≈ 41 nM.

Similarly, we found while studying the development of new bis-NTA probes that none of our synthesized Ni^{2+}-preloaded bis-NTA ligands exhibited a sub-micromolar dissociation constant towards an H_6 tag. We sought an explanation for absence of a stronger expected cooperative effect with complexation of oligohistidine tags by Ni^{2+}-preloaded bis-NTA ligands (Figure 1). Chemical flexibility of bis-NTA ligands, oligohistidine tag length (hexahistidine, H_6, and decahistidine, H_{10}), and effective generation of the expected binary bis-NTA–$(Ni^{2+})_2$ complex **A** have been explored for that purpose.

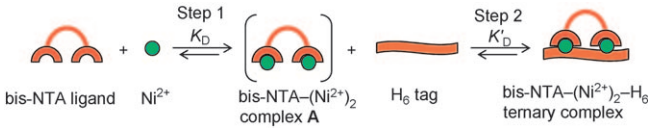

Figure 1. Schematic representation of the bis-NTA–$(Ni^{2+})_2$–H_6 ternary complex formation.

To study these parameters and the binding mechanism of bis-NTA ligands with histidine through Ni^{2+}, we synthesized new bis-NTA ligands with different structures and investigated the preorganization of these divalent chelators with nickel(II), which is the crucial step (Step 1, Figure 1) before the ternary complex formation.

In this article, mechanistic considerations are discussed based on thermodynamic characterization carried out by isothermal microcalorimetry (ITC) and fluorescence anisotropy, thereby providing new insight into the binding mode of bis-NTA ligands with Ni^{2+}. Many examples document enhanced affinities of multivalent NTA ligands for multivalent oligohistidines relative to the monovalent NTA binding module,[23,24] but the molecular mechanism that contributes to their potencies is still poorly understood.

The focus of this study lies in the comparison of new and reported data to gain an understanding of the cooperative effects, which are less than the theoretical maximum, observed in the particular case of the interaction between Ni^{2+}-preloaded bis-NTA and polyhistidines.

Results and Discussion

Prior to the design of multivalent ligands for recognizing H_6 sequences, the ability of the H_6 peptide to accept and anchor more than one NTA head needed confirmation. Theoretically, the H_6 sequence is able to bind a maximum of three independent Ni^{2+}–NTA moieties since it provides six coordination sites through the six imidazole groups.[23] However, the spatial conformational demand and constraint of the ligand might preclude the binding of several Ni^{2+}–NTA moieties. Our study therefore began with the ITC titration of a H_6 peptide with Ni^{2+}-preloaded nitrilotriacetic acid (Figure 2).

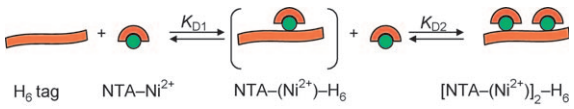

Figure 2. Titration of a H_6 oligopeptide with Ni^{2+}-preloaded mono-NTA.

Data processing of the resulting ITC binding isotherm curve (Figure 3) using a nonlinear regression model provided two affinity constants ascribed to the formation of two

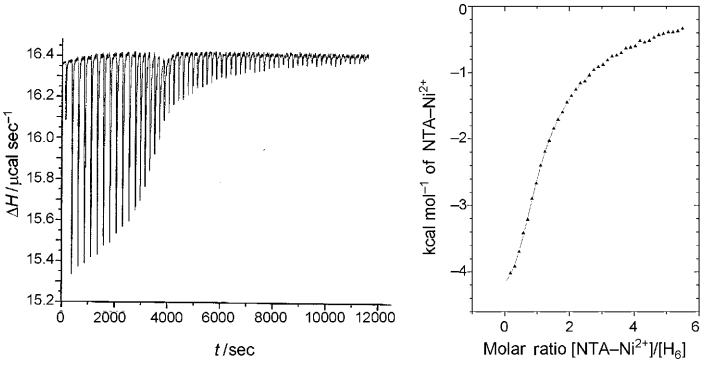

Figure 3. Raw ITC titration curve (left) and processed data (right) for the titration of H_6 oligopeptide with NTA–Ni^{2+} (100 mM Tris buffer, pH 8.0, 20 °C, [H_6] = 0.15 mM, [NTA–Ni^{2+}] = 5.55 mM). The black line corresponds to a fit of a standard interaction model assuming two binding sites.

complexes of stoichiometries 1:1 and 2:1, respectively. The smallest dissociation constant K_{D1} = 17 μM defines the most stable 1:1 NTA–Ni^{2+}–H_6 complex, whereas the second value K_{D2} = 305 μM confirms that a second Ni^{2+}–NTA moiety can bind to the same tag at the same time with lower affinity. These data not only corroborate Ebright's hypothesis that the hexahistidine tag should be able to interact with up to two Ni^{2+}–NTA moities,[20] but also justify the design of bis-NTA ligands in place of more complex supramolecules with a higher number of valencies.[19] This titration experiment provided a reference value for the stability constant of the model ternary complex NTA–Ni^{2+}–H_6 (K_D(mono-NTA) = 17 μM), which is in good agreement with data reported earlier in different buffers such as tris(hydroxymethyl)aminomethane (Tris), 4-(2-hydroxyethyl)-1-piperazineethanesulfonic acid (HEPES), and phosphates, and at different ionic strengths.[20,23,25] These results suggest that the experimental conditions used and the data analysis are in accordance with the requirements necessary to reproduce literature values for the binding constants and thermodynamic parameters.

The observed variations of the dissociation constant K_D (or $\log K_D$) values in different conditions are mainly ascribed to the pH of the medium and to the metal interaction with the buffer, which have to be taken into account and corrected if necessary.[26] For the purpose of comparison with literature data, our results were not corrected, as reported earlier.[20,23,25]

Based on this result, we designed and synthesized new bis-NTA ligands **2**–**6** (see below) (for synthetic details, see the Experimental Section) and studied the influence of their skeleton flexibility on their affinity for polyhistidine tags.

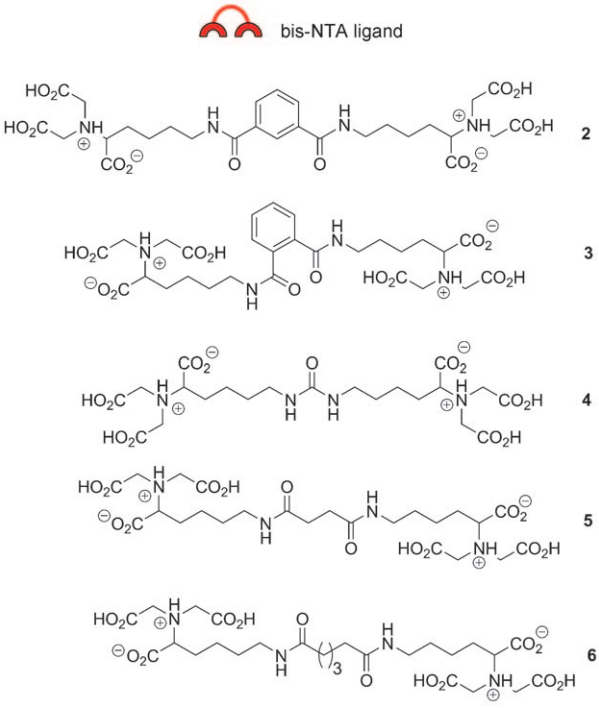

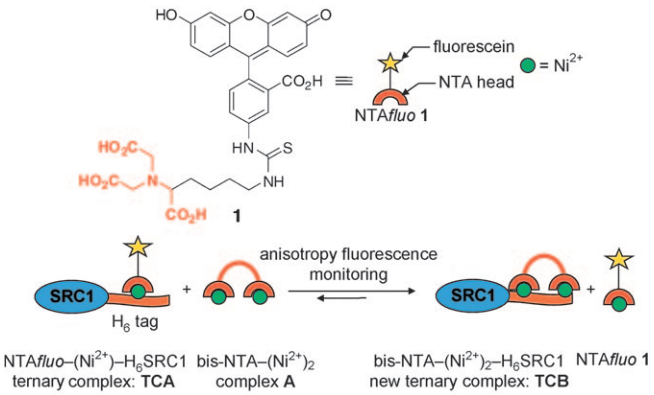

Figure 4. Structure of fluorescent probe **1** and schematic representation of the fluorescence-polarization-based competition test.

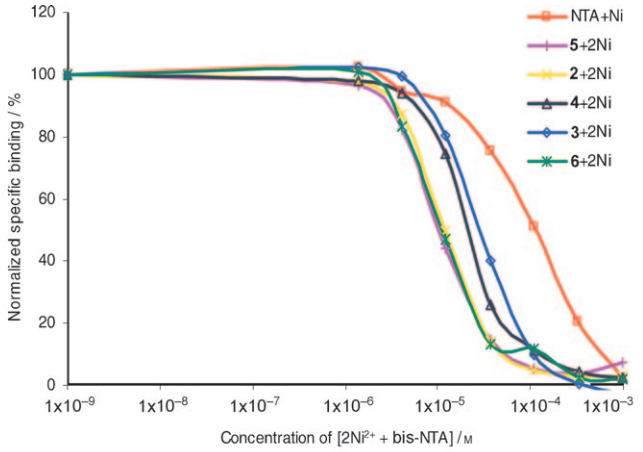

Figure 5. Fluorescence anisotropy experiments: competition curves associated with the disruption of the fluorescent ternary complex **TCA** (10 μM) by addition of increasing amounts (from 1 mM to 10 nM) of nickel-preloaded competitors (either NTA–Ni^{2+} or bis-NTA **2**–**6** preloaded with two equivalents of Ni^{2+}).

This study examines the structural complexity, the steric hindrance, and the molecular dynamics of bis-NTA ligands. The most promising bis-NTA lead was selected by a fluorescence-polarization-based competition test in which the disruption of the reference fluorescent ternary complex, that is, **1** previously bound to a H_6-tagged protein,[27] by nonfluorescent bis-NTA competitors **2**–**6** is monitored (Figure 4).

As our model anchoring protein, we selected the steroid receptor cofactor H_6SRC1 tagged by six histidine residues (H_6) on its N terminus due to its availability, stability, and structural characterization. Typical competition curves were obtained for five bis-NTA competitors **2**–**6** (Figure 5). The decrease of the fluorescent polarization signal shows the disruption of the ternary complex **TCA** and the release of the fluorescent probe NTA*fluo* into the medium, and therefore the formation of the nonfluorescent ternary complex bis-NTA–$(Ni^{2+})_2$–H_6SRC1 **TCB** (Figure 4).

Decrease of the fluorescence polarization signal occurs at lower concentrations of bis-NTA ligands than the concentration of nonfluorescent mono-NTA ligands (red curve, Figure 5). This suggests that all the ternary complexes involving bis-NTA chelators **2**–**6** are more stable than the reference NTA–Ni^{2+}–H_6SRC1 complex. Interestingly, the spatial orientation of both NTA heads fixed by the *meta*-substitution pattern of the central aromatic core of **2** was found to have a significant positive influence on the stability of the ternary complex, since ligand **2** disrupts the reference complex at lower concentration than ligand **3**, which contains an *ortho*-substitution pattern. Moreover, it is important to point out that bis-NTA ligands **5** and **6**, which bear a more flexible aliphatic central core, exhibit a comparable affinity for H_6SRC1 to the one observed for bis-NTA **2**. Additionally, our results suggested that the flexible bis-NTA **4** exhibited a lower stability for H_6SRC1 relative to **5** and **6**.

The affinity constant of the promising bis-NTA ligand **2** for the H_6-tagged protein was determined by direct-binding experiments based on fluorescence polarization measurements (Figure 6). To monitor the direct specific interaction

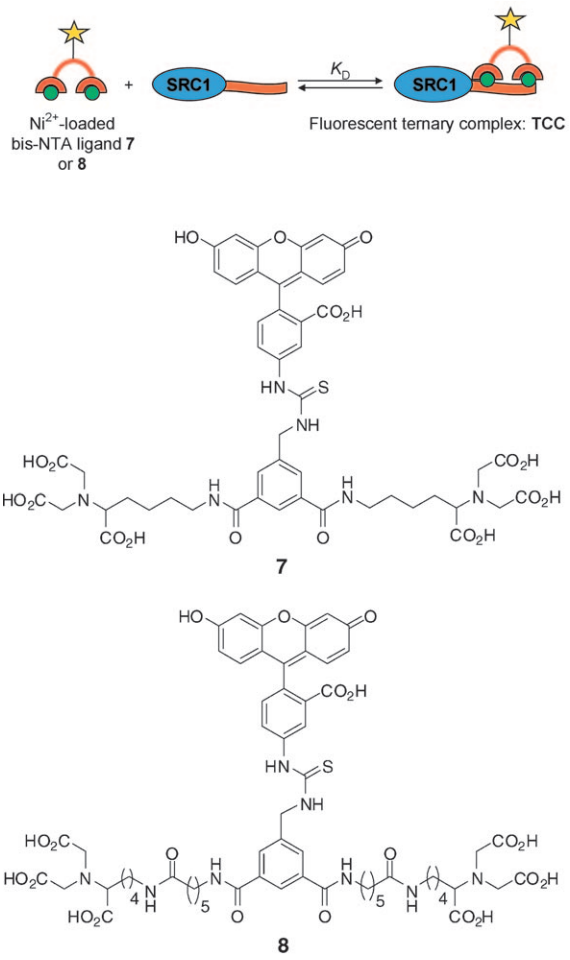

Figure 6. Schematic representation of the direct-binding test between the fluorescent bis-NTA ligands (**7** or **8**) with a hexahistidine-tagged protein, H_6SRC1, and chemical structures of the synthesized fluorescently labeled bis-NTA ligands **7** and **8**.

with the oligohistidine tag, a derivative of **2** was fluorescently labeled to give probe **7**. The analogue **8** was also prepared to study the influence of the spacer length between the NTA binders on the affinity constant with histidine tags. Details of the chemical synthesis of probes **7** and **8** (Figure 6) can be found in the Experimental Section.

The results of the direct-binding fluorescence polarization experiments involving Ni^{2+}-preloaded bis-NTA **7** and **8** with the H_6SRC1 protein are reported in Figure 7 (yellow and red curves). For bis-NTA **7** the data confirm, as previously reported, the formation of ternary complexes of higher stability compared with the reference **1**–Ni^{2+}–H_6SRC1 (Figure 7, yellow curve). However, for ligand **8** only a moderate increase in stability was detected, probably due to a higher flexibility of the spacer length (red curve). The titration of **7** yielded a K_D of 0.5 μM, which is in good agreement with the published values including those of the groups of Ebright (0.4–1 μM)[20] and Piehler and Tampé (0.27 μM)[23] for other structurally different bis-NTA chelators. Our results and the reported data suggested that the chemical flexibility and structural diversity of bis-NTA ligands may also play a

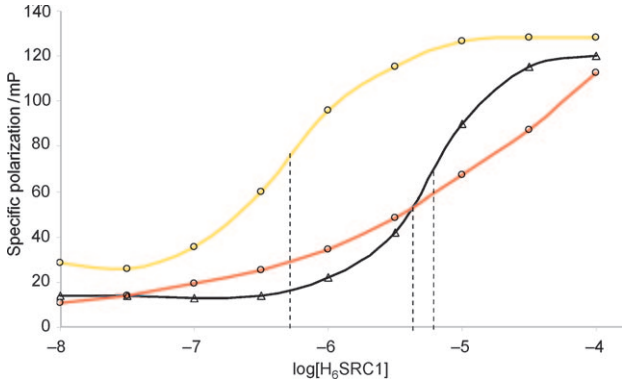

Figure 7. Determination of the affinity constants associated with **7**–$(Ni^{2+})_2$–H_6SRC1 (yellow curve) and **8**–$(Ni^{2+})_2$–H_6SRC1 (red curve) complexes by fluorescence polarization compared with reference **1**–Ni^{2+}–H_6SRC1 (blue curve).

role in the overall stability of ternary complexes; however, the structural factor seems not to influence the affinity constant for H_6-tagged proteins dramatically.

Although the best bis-NTA chelator, **7**, affords almost a 10-fold increase in affinity compared with the mono-NTA binder, **1** ($K_D(\mathbf{7}) = 0.5\ \mu M < K_D(\mathbf{1}) = 4.0\ \mu M$; see the Experimental Section), the stability remains less than the theoretical maximum and confirms that the positive cooperation effect induced by the intramolecular chelation of the second NTA head to the multivalent hexahistidine tag is limited, regardless of the skeleton and flexibility of the bis-NTA ligand.

Further ITC experiments were performed to determine the influence of polyhistidine tag length on the stability of the ternary bis-NTA–$(Ni^{2+})_2$–H_x complex ($x = 6$ or 10). These titrations showed no significant decrease of the dissociation constant ($K_D(H_6) = K_D(H_{10}) = 2\ \mu M$ (data not shown). Although Vogel et al. observed an increase in stability of the ternary complex involving a H_{10}-tagged protein,[25] our observations agree with those of Ebright, Piehler, and Tampé.[20,23,24]

Since neither structural flexibility of bis-NTA ligands nor histidine tag length has a dramatic influence on the binding affinity constant of the ternary complex,[20,23,24] one could question the formation of the bis-NTA–$(Ni^{2+})_2$ **A** entity involved in the accepted binding mechanism of Ni^{2+}-preloaded bis-NTA with oligohistidine tags (Step 1, Figure 1). Such large divalent flexible and functionalized bis-NTA ligands might oligomerize or assemble in discrete species when preloaded with nickel. Because our previous fluorescence polarization experiments did not demonstrate the presence of the bis-NTA–$(Ni^{2+})_2$ **A** entity, we assayed to monitor and to characterize better the Ni^{2+}-preloading step of bis-NTA ligands by ITC titration.

ITC study of the complexation between Ni^{2+} and bis-NTA ligands: This physical method gives a direct insight into the sequence of ligation states of Ni^{2+} during titration.[28] Data processing by a nonlinear regression model of the titration

curves generates all thermodynamic parameters describing the complexation phenomena (enthalpy ΔH, entropy ΔS, binding constant K_D, and stoichiometry n of the complex). The current study describes the results of both normal and reverse titration experiments of Ni^{2+} with bis-NTA ligands **2**–**5** (see Figure 8). We focused on the ability of bis-NTA ligands to form, through their interaction with nickel, oligomers and/or discrete species that could influence the formation of the desired ternary bis-NTA–$(Ni^{2+})_2$–H_6 complex. Knowing the hexacoordination of the nickel(II) ion and the ability of the NTA head to self-assemble around the metal ion to afford the NTA–Ni^{2+}–NTA complex,[29] the formation of several species and intermediates such as **A**–**E** could be anticipated during the titration between bis-NTA ligands and Ni^{2+} (Figure 8).

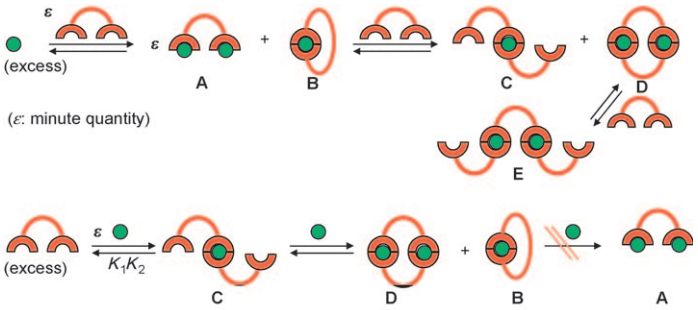

Figure 8. Top: Normal addition of bis-NTA ligand to a solution of Ni^{2+} in Tris buffer) and bottom: reverse addition of a solution of Ni^{2+} to a bis-NTA ligand solution in Tris buffer) mode of titration.

In Figure 9 the normal and reverse ITC thermograms and the associated titration curves of five different bis-NTA ligands titrated with Ni^{2+} are shown. Both the normal and reverse titration experiments were analyzed by using, respectively, the "two-site" and "deconvoluted two-site" regression models proposed from using the Origin software.[30] The results are shown in Table 1.

Quantitative analysis of normal and reverse titrations of ligand **3** with Ni^{2+} gave identical values for the thermodynamic parameters (Table 1, entry 3, $n_1 \cong 1$, $\log K_1 \cong 7.3$ and $n_2 = 2$, $\log K_2 = 4.8$), which suggests that both processes involve the formation of the same species. Since the beginning of the reverse titration unambiguously involves species **C** ($n_2 = 0.5$), the normal titration presumably also generates species **C** by "ring-opening" of species **B** and subsequent complexation with another bis-NTA molecule (Figure 8A and B). Considering the stoichiometry values n_1 and n_2 measured during normal titration, species **A**, **E**, and therefore **D** are precluded. The specific formation of the 1:1 complex **B** might be attributed to the *ortho* substitution of the central aromatic core of ligand **3**, which favors intramolecular complexation. In terms of enthalpy variation, the collected data ($\Delta H = -8$ kcal mol^{-1}) match values recently reported by our group for the complexation between two independent mono-NTA and Ni^{2+} (entries 1, 2, and 5 in Table 2).[29]

In contrast, normal and reverse titration of bis-NTA **2**, **4**, and **5** lead to different enthalpy values. This result implies that normal and reverse additions involve different binding modes and therefore generate different species. In these particular cases in which the binding mode proves to be nonreversible, the "deconvoluted two-sites" model is known to be inappropriate.[31] Therefore, in the case of bis-NTA **2**, **4**, and **5** only the normal addition mode should be considered for quantitative description. The successful "two-sites" regression, which displays stoichiometries of average values of $n_1 \cong 0.8$ and $n_2 \cong 1.5$, suggests the concomitant formation of the species **A**, **B**, and **D** in the first equilibrium, and the generation of less stable species, such as **C** and **E**, when additional bis-NTA ligands are added (normal titration, Figure 8A). In the first equilibrium, species **B** and **D** predominate over **A**, as suggested by the stoichiometry n_1 being close to 1 (1:1 or 2:2 complex). In the reverse mode of addition, after the addition of more than one equivalent of nickel, no enthalpy change is observed (Figure 9A). This result implies that the intended bis-NTA–$(Ni^{2+})_2$ complex **A** is not generated at all, even when an excess of Ni^{2+} is added to the bis-NTA solutions (step 3, Figure 8B).

Our study strongly suggests that the standard procedure for Ni^{2+} preloading of bis-NTA ligands does not lead to the exclusive formation of the claimed species **A**, but rather affords a mixture of discrete complexes **A**, **D**, and **B**. This observation is supported by the result of nickel estimations performed on the presumed bis-NTA–$(Ni^{2+})_2$ complex synthesized by Ebright et al., since a 1.4 ratio was obtained for the complex nickel(II)/bis-NTA instead of 2.[20] This relative lack of Ni^{2+} reveals the formation of species that have a lower concentration of nickel than expected, thus leaving uncomplexed or free Ni^{2+} in the solution. A proposed mechanism for the formation of these ternary complexes is now needed. Figure 10 shows the postulated pathway with stepwise formation of ternary complexes between H_6 tags and Ni^{2+}-preloaded bis-NTA ligands. Since we have shown that **D** and **B** are preferentially formed, it is assumed that the addition of the multivalent histidine tags onto these Ni^{2+}-preloaded bis-NTA complexes triggers dissociation of the most labile NTA head of **D** or **B**, thereby generating open structures such as **F** and **G**. Chelation of the two remaining valencies of the nickel ion by two imidazole residues of the histidine tag follows, thereby affording the ternary complexes **H**, **I**, and **J** (Figure 10). The concomitant generation of less stable complexes **H** and **I** can explain the limited increase in stability for all ternary complexes involving polyhistidine and bis-NTA ligands. The apparent affinity constant measured here for bis-NTA–$(Ni^{2+})_2$–H_6 and published values are averages of all stability constants associated with ternary complexes such as **H**, **I**, and **J**.

To demonstrate the presence of free or uncomplexed Ni^{2+} due to the formation of species such as **B** and **D**, and to support the mechanism proposed in Figure 10, the H_6 peptide was titrated by ITC with our bis-NTA ligands **2**–**5** initially preloaded with exactly one or two equivalents of Ni^{2+}. When two equivalents of Ni^{2+} were used for the loading of

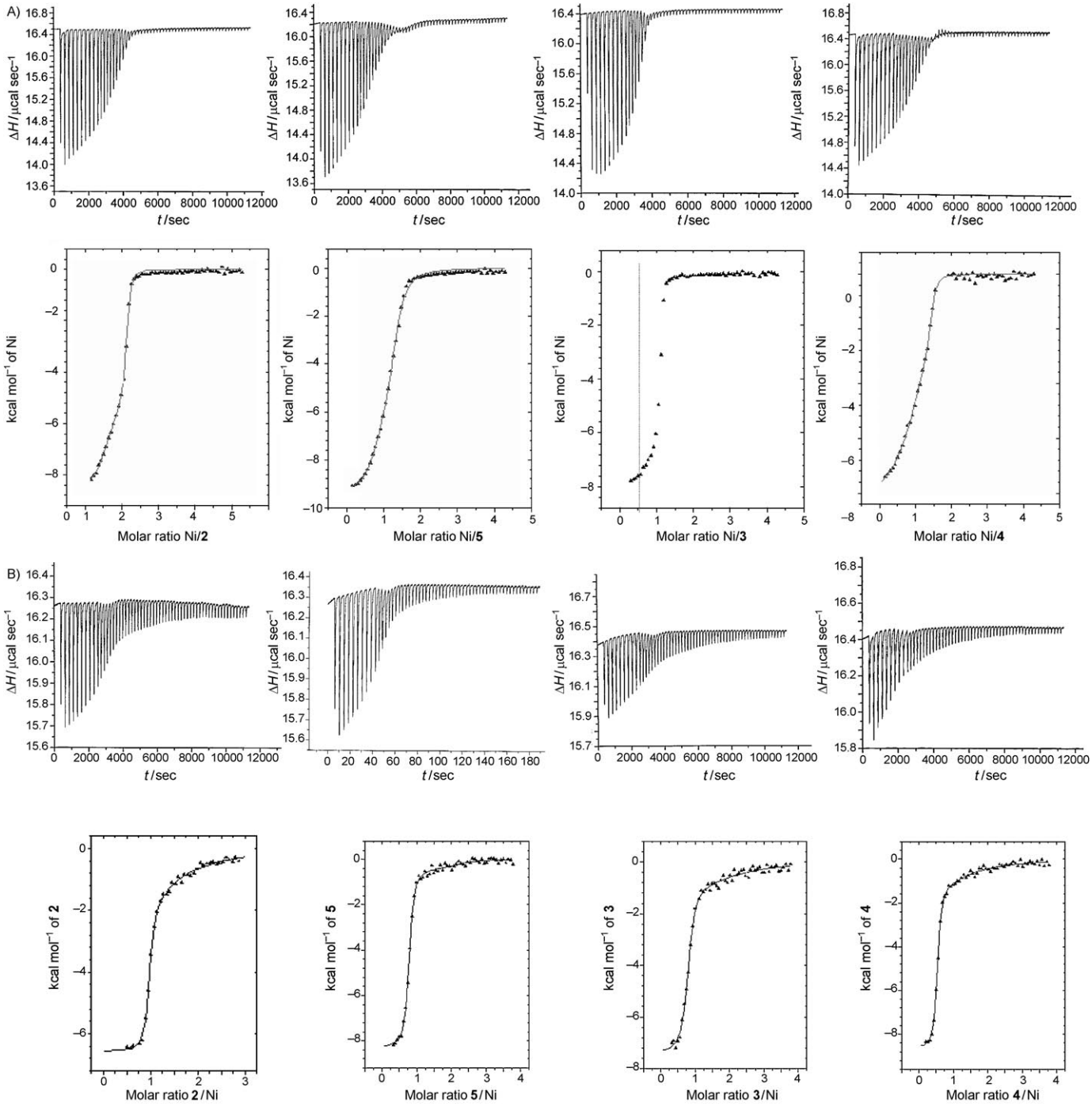

Figure 9. A) ITC thermograms (top) and reverse titration curves (bottom) of bis-NTA chelators **2**–**5** with Ni^{2+} (100 mM Tris buffer, pH 8.0, 20 °C, [bis-NTA] = 0.09 mM, $[Ni^{2+}]$ = 1.70 mM). All collected data were analyzed using a deconvoluted "two-site" binding model. B) ITC thermograms (top) and normal titration curves (bottom) of Ni^{2+} with bis-NTA chelators **2**–**5** (100 mM Tris buffer, pH 8.0, 20 °C, [bis-NTA] = 0.5 mM, $[Ni^{2+}]$ = 0.03 mM). All collected data were analyzed using a standard "two-site" binding model.

2–**5** (Figure 11), the corresponding titration curves display a highly exothermic interaction in the range of 9 to 15 kcal mol^{-1} of injectant at the very beginning of the titration. However, when one equivalent of Ni^{2+} is used (Figure 12, left part), lower enthalpy changes accompany the formation of the ternary complex with H_6 (3.5 kcal mol^{-1}). The difference between enthalpy values suggests that most of the energy evolved at the beginning of the titration of the H_6 peptide by bis-NTA chelators **2**–**5** preloaded with two equivalents of nickel (9 to 15 kcal mol^{-1}) should be assigned to a separate kind of interaction. We found this interaction ascribable to direct interaction of the "free nickel(II)" with

Table 1. Thermodynamic data derived from the ITC normal and reverse curves using, respectively, the deconvoluted two-site model and the two-site binding model.

Entry	Bis-NTA	Reverse titration (deconvoluted "two sites" model)						Normal titration ("two sites" model)					
		n_1	$\log K_1$	ΔH_1[a]	n_2	$\log K_2$	ΔH_2[a]	n_1	$\log K_1$	ΔH_1[a]	n_2	$\log K_2$	ΔH_2[a]
1	**2**	0.9 (Ni/**2**)	7.2	−7553	0.8 (Ni/**2**)	4.5	−2668	0.9 (**2**/Ni)	7.0	−6561	1.4 (**2**/Ni)	4.4	−5197
2	**4**	0.8 (Ni/**4**)	6.7	−10570	0.6 (Ni/**4**)	4.9	−2020	0.8 (**4**/Ni)	7.9	−8306	2.1 (**4**/Ni)	5.5	−497
3	**3**	0.9 (Ni/**3**)	7.3	−8000	0.50 (Ni/**3**)	4.8	−1200	0.8 (**3**/Ni)	7.0	−7400	2.3 (**3**/Ni)	4.8	−1200
4	**5**	0.7 (Ni/**5**)	7.0	−7947	0.4 (Ni/**5**)	4.4	−6859	0.5 (**5**/Ni)	7.0	−8628	1.3 (**5**/Ni)	4.7	−2770

[a] Units of cal mol^{-1}.

Table 2. Theoretical calculation of association enthalpies related to species 2:1, 1:1, and 2:2 based on published enthalpy values associated with complexes Ni^{2+}–NTA and NTA–Ni^{2+}–NTA.[30]

Entry	Complex	Reaction equilibrium	Association enthalpy (ΔH_F)	ΔH_F of ligand [kcal mol^{-1}]
1		Ni+NTA⇌Ni–NTA	ΔH_1	−6.5[30]
2		Ni–NTA+NTA⇌NTA–Ni–NTA	ΔH_2	−1.5[30]
3		2 Ni+bis-NTA⇌bis-NTA–$(Ni)_2$	$\Delta H = 2\Delta H_1$	−13
4	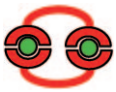	2 Ni+2 bis-NTA⇌$[bis\text{-}NTA\text{–}Ni]_2$	$\Delta H = (2\Delta H_1 + 2\Delta H_2)/2$	−8
5		Ni+bis-NTA⇌bis-NTA–Ni	$\Delta H = \Delta H_1 + \Delta H_2$	−8

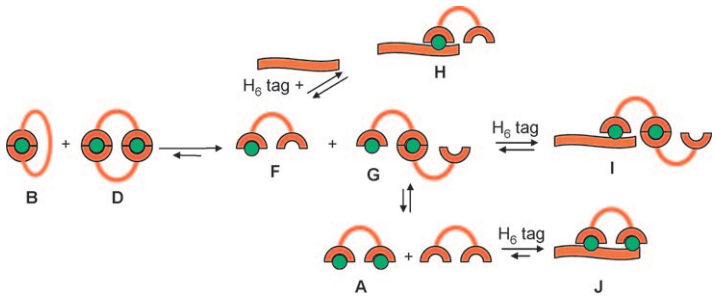

Figure 10. Postulated mechanism for the formation of ternary complexes **H**, **I**, and **J** with histidine tags, starting from species **B** and **D**.

the hexahistidine tag itself. ITC monitoring of the enthalpy variation during titration of Ni^{2+} by H_6 oligopeptide (Figure 12, right part) displays an enthalpy variation (12 kcal mol^{-1}) of the same order of magnitude as observed during the ternary complex formation in the presence of two equivalents of nickel. This observation led us to investigate further the (Ni^{2+})/oligohistidine interaction by calorimetry. The results of this study will be reported in a separate publication. Confirmation of the presence of unbound nickel(II) ion validates our hypothesis that bis-NTA–$(Ni^{2+})_2$ is not formed preferentially during the preloading step of bis-NTA ligands, and supports the proposed mechanism for the formation of ternary complexes.

In spite of the observed complication at the beginning of the ITC titration, the curves shown in Figure 11 were used to determine the affinity constant of the ternary complex. As the initial part of the curve corresponds to the exothermic interaction between free nickel and oligohistidine peptide, the first eight data points were deleted to analyze the ternary complex quantitatively. The deletion has little influence on the fit of experimental data belonging to the later portion of the curve, as evidenced by Anslyn et al.[32] An excellent fit to the curve was obtained using the sequential two-site model. The success of this model suggests that two distinct species with stoichiometries of 1:1 and 2:1 are formed by successive fixation of one followed by a second bis-NTA chelator onto the hexahistidine multivalent platform. The apparent affinity constant K_D of the 1:1 entity, namely, **H**, **I**, or **J** falls between 2 and 9 μM for ligands **2** and **3**, respectively. These quite modest affinity values, which are of the same order of magnitude as those previously measured with ligand **7** and H_6SRC1, confirm that species like **F** and **G** predominate over **A**, thereby precluding positive cooperative effects.

Conclusion

By means of isothermal calorimetry and fluorescence anisotropy, we studied the formation of ternary complexes between Ni^{2+}-preloaded NTA and bis-NTA ligands with either H_6 or H_6SRC1. In agreement with published data, our studies involving bis-NTA ligands showed only limited increase in stability regarding the formation of ternary complexes with H_6SRC1. Based on these results, we propose that the absence of a strong cooperative effect is mainly due to the propensity of the divalent molecules to form discrete species and oligomers. Preloading of bis-NTA ligands with two equivalents of Ni^{2+} does not exclusively provide the usually postulated bis-NTA–$(Ni^{2+})_2$ species **A** required for the effective site-selective labeling of H_6-tagged proteins. Instead, discrete species such as **B** and **D** with defined stoichiometries are generated and have been characterized by using

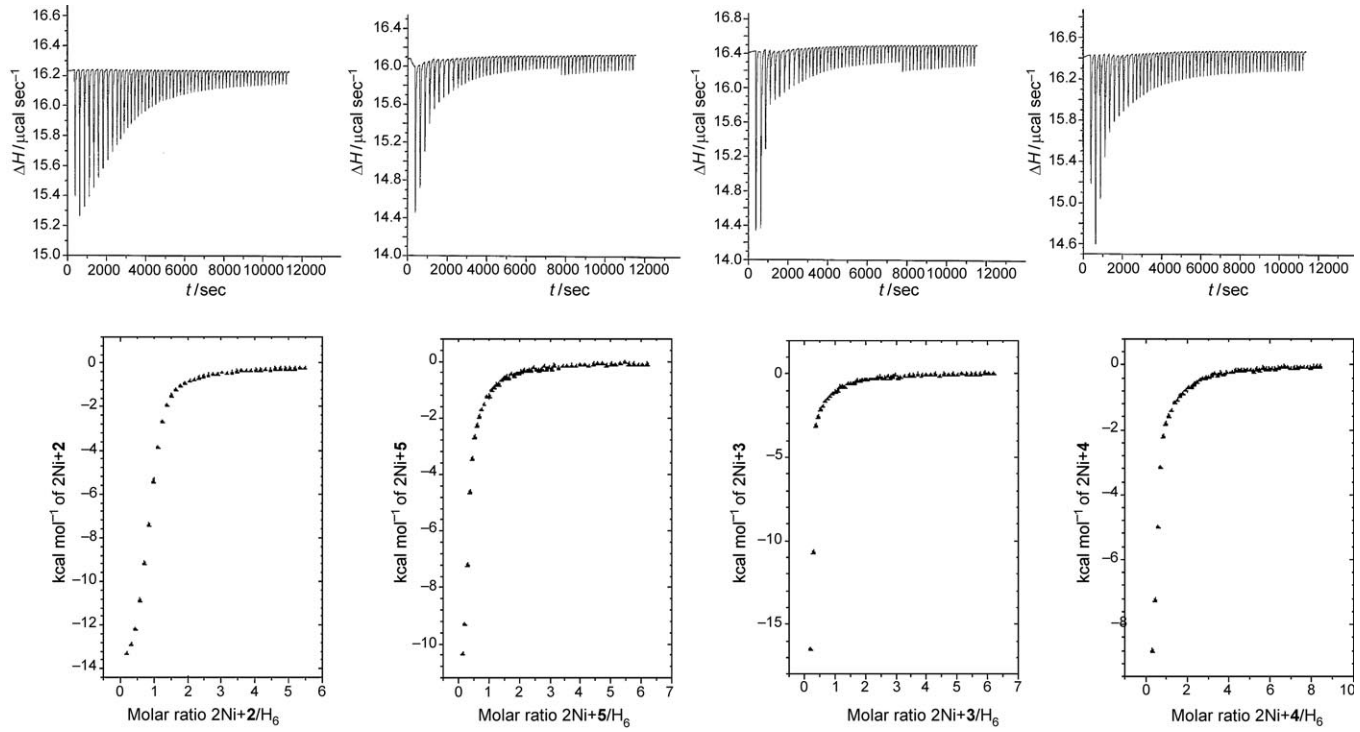

Figure 11. ITC thermograms and titration curves of H_6 peptide with bis-NTA chelators **2**–**5** preloaded with two equivalents of nickel(II) (100 mM Tris buffer, pH 8.0, 20 °C, $[(Ni^{2+})_2$–bis-NTA$] = 1.85$ mM, $[H_6] = 0.05$ mM). All collected data were analyzed using a sequential two-site binding model.

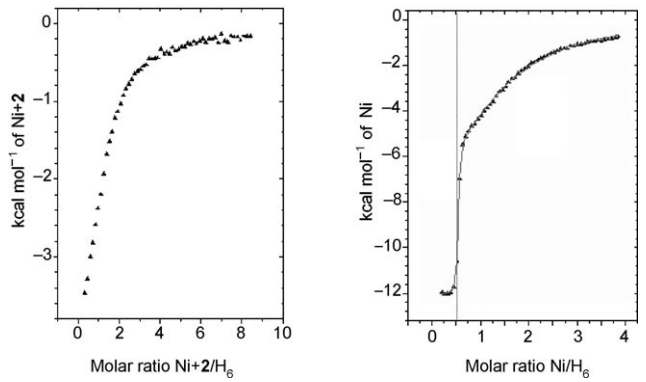

Figure 12. Left) Titration curve of H_6 peptide with bis-NTA chelators **2** preloaded with only one equivalent of nickel(II) (100 mM Tris buffer, pH 8.0, 20 °C, $[Ni^{2+}$–**2**$] = 1.85$ mM, $[H_6] = 0.05$ mM). Right) Titration curve of H_6 peptide with nickel(II) (100 mM Tris buffer, pH 8.0, 20 °C, ligands **3**–**5**: $[Ni^{2+}] = 2.55$ mM, $[H_6] = 0.15$ mM).

ITC. As a consequence, the apparent affinity constant measured experimentally for the expected unique ternary complex **J** includes a contribution from the less stable ternary complexes **H** and **I**, which masks the cooperative effect expected for the chelation of bis-NTA–$(Ni^{2+})_2$ complex **A** with the hexahistidine tag. A rational mechanism has been postulated for the generation of ternary complexes **H**, **I**, and **J** from species **F** and **G**. In light of our studies, the specific behavior of bis-NTA ligands towards Ni^{2+} should be taken into account regarding more complex multivalent NTA ligands such as tris- and tetra-NTA. ITC experiments investigating the interaction of bis-NTA ligands preloaded with two equivalents of nickel with hexahistidine peptides revealed a strong affinity of nickel for the hexahistidine sequence. These observations led us to consider polyhistidines tags as new reversible ligands for the site-selective labeling of histidine-tagged proteins. These studies will be published in due course.

Experimental Section

Chemical synthesis of bis-NTA ligands: Experimental procedures leading to the nonfluorescent bis-NTA ligands **2**, **3**, **5** and to fluorescein bis-NTA probes **7** and **8** are provided here. ^1H and ^{13}C NMR spectroscopy of all new compounds are given in the Supporting Information. Fluorescent probe **1** was synthesized as described in the literature.[33] Ligands **4** and **6** were a kind gift from Dr. C. Richard (CEA, Saclay, France).

All reactions were performed in oven-dried glassware under an argon atmosphere unless otherwise stated. The following solvents were distilled from the indicated drying agents: CH_2Cl_2 (CaH_2), THF (Na), CH_3CN (CaH_2), or dried over 4 Å molecular sieves. All commercially available reagents were used without further purification. Analytical thin-layer chromatography (TLC) was performed using glass-backed silica gel plates. Visualization of the developed chromatogram was performed using UV absorbance and a vanillin solution. Flash column chromatography was performed with silica gel (40–63 μm) according to a standard technique. Nuclear magnetic resonance spectra (^1H and ^{13}C) were recorded using 200, 300, and 400 MHz spectrometers equipped with a broadband inverse detection (BBI) or a dual probe. Chemical shifts for ^1H and ^{13}C spectra are recorded in parts per million (ppm) using the residual chloroform as internal standard (^1H, $\delta = 7.26$ ppm; ^{13}C, $\delta = 77.16$ ppm).

Multiplicities are indicated by s (singlet), brs (broad singlet), d (doublet), t (triplet), q (quadruplet), qt (quintuplet) and m (multiplet). Coupling constants, *J*, are reported in Hz. Mass spectra were recorded using MS/MS high-resolution Micromass ZABSpecTOF spectrometry. Infrared spectra were recorded using a FTIR spectrometer equipped with KRS-5 (ThI/ThBr) lenses and are reported in reciprocal centimeters (cm^{-1}).

2-[Bis(carboxymethylamino)]-6-*tert*-butoxycarbonylaminohexanoic acid (10): A 2 M NaOH solution (15.2 mL, 30.4 mmol, 3.0 equiv) containing N^{ε}(*tert*-butoxycarbonyl)-L-lysine (2.5 g, 10.1 mmol, 1.0 equiv) was added dropwise to a 2 M sodium hydroxide solution (10.1 mL, 20.2 mmol, 2.0 equiv) of bromoacetic acid (2.82 g, 20.2 mmol, 2.0 equiv) over 1 h at 0 °C. The reaction mixture was stirred at 0 °C for 2 h and then at 50 °C for 16 h. After cooling at 0 °C, the pH of the reaction was kept at 2 by careful and slow addition of concentrated HCl. The reaction vessel was then left at 5 °C overnight and the desired triacid was obtained as a white precipitate, which was filtered and dried by lyophilization, thereby affording **10** as a white powder (2.39 g, 6.6 mmol, 65 %). ^{1}H NMR (CD_3OD, 300 MHz): δ = 3.65 (brs, 4H), 3.49 (t, J = 6.8 Hz, 1H), 3.07 (m, 2H), 1.90–1.60 (m, 6H), 1.46 ppm (brs, 9H); ^{13}C NMR (D_2O/CD_3OD, 75.5 MHz): δ = 176.7, 159.3, 80.7, 67.5, 56.2, 41.9, 31.6, 31.4, 29.7, 25.5 ppm; IR (KBr): $\tilde{\nu}$ = 3406, 2979, 2541, 2343, 1957, 1891, 1693, 1530, 1395, 1369, 1256, 1170, 1061, 987, 783, 713, 682, 577, 440 cm^{-1}; MS (ES): unknown fragmentation.

2-[Bis(benzyloxycarbonylmethylamino)]-6-*tert*-butoxycarbonylaminohexanoic benzyl ester (11): Benzyl bromide was added dropwise to a solution of **10** (1.21 g, 3.34 mmol, 1.0 equiv) in anhydrous DMF (25 mL) in the presence of cesium carbonate (6.52 g, 20.0 mmol, 6.0 equiv). The reaction mixture was then warmed at 65 °C for 24 h. After cooling at room temperature, the reaction was quenched by addition of a saturated aqueous solution of ammonium chloride (25 mL) and extracted with diethyl ether. The organic phase was then dried over $MgSO_4$, filtrated, and evaporated to dryness. The residue was purified by column chromatography on silica gel, thereby affording **11** as a yellow oil (1.07 g, 1.69 mmol, 51 %). ^{1}H NMR ($CDCl_3$, 300 MHz): δ = 7.32 (brs, 15H), 5.08 (brs, 6H), 4.54 (brs, 1H), 3.70 (brs, 4H), 3.46 (t, J = 6.8 Hz, 1H), 3.02 (brs, 2H), 1.75–1.60 (m, 4H), 1.50–1.30 ppm (m, 11H); ^{13}C NMR ($CDCl_3$, 50 MHz): δ = 172.7, 171.4, 156.1, 136.0, 135.9, 128.7, 128.5, 79.1, 66.6, 65.0, 52.9, 40.5, 30.4, 29.7, 28.7, 23.3 ppm; IR (CsI): $\tilde{\nu}$ = 3405, 3034, 2934,1746, 1511, 1500, 1455, 1366, 1249, 1166, 992, 747, 698, 607, 475, 406 cm^{-1}; MS (ES): m/z (%): 633 (10) $[M+H]^+$, 655 (100) $[M+Na]^+$, 671 (90) $[M+K]^+$.

6-Amino-2-[bis(benzyloxycarbonylmethylamino)]hexanoic benzyl ester (12): Compound **11** (600 mg, 0. 95 mmol, 1.0 equiv) was dissolved in CH_2Cl_2 (35 mL) containing trifluoroacetic acid (5 mL, 64.9 mmol, 68 equiv). The homogeneous solution was then stirred at room temperature for 4 h and evaporated to dryness. The remaining trifluoroacetic acid was removed by codistillation with toluene to give the trifluoroacetic acid (TFA) salt of the desired product as an oil (720 mg, 0.95 mmol, 100 %). ^{1}H NMR ($CDCl_3$, 200 MHz): δ = 7.88 (brs, 2H), 7.30 (brs, 15H), 5.07 (brs, 6H), 3.60 (brs, 4H), 3.47 (m, 1H), 3.05–2.90 (m, 2H), 1.80–1.50 ppm (m, 6H); ^{13}C NMR ($CDCl_3$, 75.5 MHz): δ = 172.5, 171.8, 137.3, 128.8, 128.6, 128.5, 128.4, 66.7, 64.4, 53.1, 39.9, 29.6, 26.5, 22.4 ppm; MS (ES): m/z (%): 533 (100) $[M+H]^+$.

6-(3-{5-Benzyloxycarbonyl-5-[bis(benzyloxycarbonylmethylamino)]pentylcarbamoyl}benzoylamino)-2-[bis(benzyloxycarbonylmethylamino)]hexanoic benzyl ester (14): Bis-*N*-succinyl isophthalic ester was added to a solution of **12** (1.60 g, 2.1 mmol, 4.6 equiv) in anhydrous CH_2Cl_2 (13 mL) in the presence of diisopropylethylamine (731 μL, 4.2 mmol, 4.6 equiv).[34] The reaction mixture was then stirred at room temperature under an argon atmosphere for 12 h, quenched with a saturated aqueous solution of ammonium chloride, dried over $MgSO_4$, filtered, and evaporated to dryness. Purification of the residue by column chromatography on silica gel afforded the desired compound as an oil (652 mg, 0.54 mmol, 60 %). ^{1}H NMR (CD_3OD, 200 MHz): δ = 8.26 (s, 1H), 7.95 (d, J = 7.8 Hz, 2H), 7.52 (t, J = 7.8 Hz, 1H), 7.40–7.20 (m, 30H), 5.03 (brs, 12H), 3.69 (brs, 8H), 3.50 (t, J = 7.8 Hz, 2H), 3,30 (m, 4H), 1.85–1.40 ppm (m, 12H); ^{13}C NMR ($CDCl_3$, 100 MHz): δ = 172.4, 171.3, 169.9, 135.6, 135.5, 134.7, 130.3, 128.6, 128.5, 128.3, 128.2, 128.0, 66.3, 64.3, 52.8, 39.8, 29.6, 28.3, 22.9 ppm; MS (ES): m/z (%): 1195 (100) $[M+H]^+$, 1217 (20) $[M+Na]^+$.

Compound 2: Compound **14** (100 mg, 9 mmol, 1 equiv) was dissolved in methanol (2 mL) in the presence of palladium on carbon (10 %, 10 mg). The reaction mixture was vigorously stirred under a hydrogen atmosphere (1 atm) at room temperature for 12 h. After completion of the reaction, the catalyst was filtered by using Celite and washed several times with methanol. Concentration of the methanol phase under vacuum followed by addition of diethyl ether, filtration, and drying gave **2** as a pure white powder (49 mg, 0.75 mmol, 86 %). ^{1}H NMR (CD_3OD, 200 MHz): δ = 8.27 (s, 1H), 7.97 (d, J = 7.8 Hz, 2H), 7.56 (t, J = 7.8 Hz, 1H), 3.70–3.55 (brs, 8H), 3.55–3.45 (m, 2H), 3.55–3.30 (m, 4H), 1.95–1.40 ppm (m, 12H); ^{13}C NMR (CD_3OD, 100 MHz): δ = 175.9, 169.5, 136.3, 131.2, 129.8, 127.1, 66.7, 55.3, 40.8, 30.7, 30.0, 24.8 ppm; MS (ES/APCI): m/z (%): 655 (not determined) $[M+H]^+$.

Phthalic acid bis(2,5-dioxopyrrolidin-1-yl) ester (13): Phthalic acid (1.0 g, 6.01 mmol, 1.0 equiv), *N*-hydroxysuccinimide (NHS; 1.66 g, 14.4 mmol, 2.4 equiv) and *N*,*N*-dicyclohexylcarbodiimide (DCC; 2.98 g, 14.4 mmol, 2.4 equiv) were dissolved in anhydrous THF (180 mL) and the reaction mixture was stirred for 12 h at room temperature. The white precipitate was then removed by filtration and the filtrate was evaporated to dryness. The crude material was dissolved in CH_2Cl_2 and treated with a saturated aqueous solution of ammonium chloride, dried over $MgSO_4$, filtered, and evaporated to dryness. Purification of the residue by column chromatography on silica gel afforded the title compound **13** as a white solid (259 mg, 0.75 mmol, 12 %). ^{1}H NMR ($CDCl_3$, 200 MHz): δ = 8.09, 7.79 (m, 4H), 2.89 ppm (brs, 8H).

6-(2-{5-Benzyloxycarbonyl-5-[bis(benzyloxycarbonylmethylamino)]pentyl carbamoyl}benzoylamino)-2-[bis(benzyloxycarbonylmethylamino]hexanoic benzyl ester (15): The phthalic ester **13** (150 mg, 0.42 mmol, 1.0 equiv) was added to a solution of **12** (300 mg, 1 mmol, 2.4 equiv) and diisopropylethylamine (348 μL, 2 mmol, 4.8 equiv) in anhydrous CH_2Cl_2 (6 mL). The resulting mixture was stirred at room temperature under an argon atmosphere for 12 h, quenched with a saturated aqueous solution of ammonium chloride, dried over $MgSO_4$, filtered, and evaporated to dryness. Purification of the residue by column chromatography on silica gel afforded the desired compound as a colorless oil (220 mg, 0.18 mmol, 44 %).^{1}H NMR ($CDCl_3$, 300 MHz): δ = 7.60–7.45 (m, 4H), 7.35 (brs, 30H), 7.13 (m, 2H), 5.25–5.00 (m, 12H), 3.73 (brs, 8H), 3.52 (t, J = 7.5 Hz, 2H), 3.34 (m, 4H), 1.85–1.45 ppm (m, 12H); ^{13}C NMR ($CDCl_3$, 75.5 MHz): δ = 172.9, 171.6, 169.6, 136.2, 136.0, 130.3, 128.7, 128.6, 66.8, 65.0, 53.2, 40.2, 30.3, 29.1, 23.5 ppm; IR (film): $\tilde{\nu}$ = 3316, 2933, 1740, 1637, 1546, 1455, 1262, 1154, 990, 976, 747, 699, 593 cm^{-1}; MS (ES): m/z (%): 1217 (100) $[M+Na]^+$.

Compound 3: A 1 M aqueous potassium hydroxide solution (2.26 mL, 2.26 mmol, 18 equiv) was added dropwise to a solution of **15** (150 mg, 126 μmol, 1.0 equiv) in methanol (12 mL) under an argon atmosphere. The resulting mixture was stirred at room temperature for 12 h and then concentrated under vacuum. The residue was treated with water (1 mL) before adding, at 0 °C, a 10 % aqueous solution of HCl to reach pH 2. The solution was concentrated under vacuum and EtOH (2 mL) was added. The resulting mixture was filtered and the filtrate was evaporated to dryness to afford a white solid. After several washings with CH_2Cl_2, **3** was obtained as an HCl salt (32 mg, 44 μmol, 35 %). ^{1}H NMR (CD_3OD, 300 MHz): δ = 8.00–7.40 (m, 4H), 3.79 (brs, 8H), 3.75–3.65 (m, 2H), 3.50–3.30 (m, 4H), 2.05–1.55 ppm (m, 12H); ^{13}C NMR (CD_3OD, 75.5 MHz): δ = 173.9, 172.6, 170.2, 133.3, 132.3, 131.1, 130.5, 129.4, 68.2, 56.4, 40.2, 28.2, 27.8, 24.6 ppm; IR (KBr): $\tilde{\nu}$ = 3433, 3036, 2627, 1704, 1638, 1398, 1275, 907, 786 cm^{-1}.

6-(3-{5-Benzyloxycarbonyl-5-[bis(benzyloxycarbonylmethylamino)]pentylcarbamoyl}-propionylamino)-2-[bis(benzyloxycarbonylmethylamino]-hexanoic benzyl ester (16): Succinic acid (21 mg, 0.18 mmol, 1.0 equiv) and benzotriazole-1-yl-oxytris(dimethylamino)phosphonium hexafluorophosphate (BOP) reagent (175 mg, 0.39 mmol, 2.2 equiv) previously dissolved in CH_2Cl_2 (3 mL) were successively added to a solution of **12** (300 mg, 0.39 mmol, 2.2 equiv) and diisopropylethylamine (138 μL, 0.79 mmol, 4.4 equiv) in anhydrous CH_2Cl_2 (6 mL). The resulting mixture was stirred at room temperature under an argon atmosphere for 12 h and quenched with a saturated aqueous solution of ammonium chloride. The organic phase was then washed with a saturated aqueous $NaHCO_3$ solu-

tion, dried over $MgSO_4$, filtered, and evaporated to dryness. Purification of the residue by column chromatography on silica gel afforded the desired compound as a colorless oil (149 mg, 0.13 mmol, 73%). ^{1}H NMR ($CDCl_3$, 200 MHz): δ = 7.34 (brs, 30H), 6.44 (m, 2H), 5.10 (brs, 12H), 3.72 (brs, 8H), 3.52 (t, J = 7.6 Hz, 2H), 3.16 (m, 4H), 2.50 (brs, 4H), 1.85–1.20 ppm (m, 12H); ^{13}C NMR ($CDCl_3$, 50 MHz): δ = 172.5, 172.4, 171.2, 135.7, 128.6, 128.3, 66.4, 64.5, 52.8, 39.2, 31.9, 29.8, 28.6, 23.0 ppm; IR (CsI): $\tilde{\nu}$ = 3304, 3034, 2941, 1745, 1647, 1546, 1456, 1262, 1208, 1154, 993, 915, 741, 698, 579, 495 cm^{-1}; MS (ES): m/z (%): 1169 (100) $[M+Na]^+$.

Compound 5: Pd/C (10%, 15 mg) was added to a solution of **16** in methanol (15 mL) under argon. The reaction mixture was placed under an atmosphere of hydrogen at room temperature and vigorously stirred for 6 h. The catalyst was then removed by filtration and the filtrate was evaporated to dryness. The residue was treated with an excess of diethyl ether, which induced the precipitation of a fine white powder (71 mg, 0.12 mmol, 86%) with a satisfactory purity. ^{1}H NMR (CD_3OD, 300 MHz): δ = 3.65–3.60 (m, 8H), 3.50 (m, 2H), 3.15 (m, 4H), 2.42 (s, 4H), 1.75–1.55 ppm (m, 12H); ^{13}C NMR (D_2O, 75.5 MHz): δ = 175.0, 174.7, 174.0, 67.1, 55.5, 39.5, 29.8, 29.6, 24.5, 26.2 ppm; MS (ES): m/z (%): 607 (16) $[M+H]^+$, 629 (100) $[M+Na]^+$.

5-(*tert*-Butoxycarbonylaminomethyl)diethyl isophthalic ester (18): Azide **17** (1.50 g, 5.42 mmol, 1.0 equiv; prepared following Powell's procedure)[35] was dissolved in anhydrous diethyl ether (37 mL). The slow addition of tributylphosphine (1.49 mL, 5.96 mmol, 1.1 equiv) under argon to the reaction mixture was accompanied by the evolution of nitrogen. The reaction mixture was then stirred for 45 min at room temperature and then frozen to −50 °C. A solution of dicarbonate di-*tert*-butyl (1.30 g, 5.96 mmol, 1.1 equiv) in diethyl ether (18 mL) was then added dropwise over 10 min. The medium was stirred for 1 h at −50 °C and quenched with a saturated aqueous solution of $NaHCO_3$ (18 mL). The reaction mixture was then extracted with diethyl ether at room temperature. The organic phase was dried with $MgSO_4$, filtered, and evaporated to dryness. The residue was then purified by column chromatography on silica gel to afford the title compound **18** as a white solid (1.47 g, 4.2 mmol, 77%). ^{1}H NMR ($CDCl_3$, 300 MHz): δ = 8.58 (s, 1H), 8.14 (s, 2H), 4.99 (m, 1H), 4.41 (s, 2H), 4.41 (q, J = 7.2 Hz, 4H), 1.48 (s, 9H; H), 1.42 ppm (t, J = 7.2 Hz, 6H); ^{13}C NMR ($CDCl_3$, 50 MHz): δ = 166.1, 156.3, 140.5, 132.8, 131.7, 130.0, 80.3, 61.8, 44.4, 28.8, 14.8 ppm; IR (film CsI): $\tilde{\nu}$ = 2981, 2936, 1724, 1523, 1370, 1322, 1244, 1172, 1030, 864, 757, 432 cm^{-1}; MS (ES): m/z (%): 374 (100) $[M+Na]^+$.

5-(*tert*-Butoxycarbonylaminomethyl)isophtalic acid (19): A solution of **18** (1.36 g, 3.87 mmol, 1.0 equiv) in methanol (80 mL) was treated with LiOH (1.14 g, 47.7 mmol, 12 equiv) previously dissolved in water (40 mL). The reaction mixture was stirred at 45 °C for 15 h. The methanol was then evaporated and the aqueous phase was extracted with diethyl ether. The aqueous layer was then acidified with a 1 M aqueous solution of HCl at 0 °C until pH 3–4 was reached and precipitation of the desired product occurred (1.02 g, 3.46 mmol, 89%). ^{1}H NMR (CD_3OD, 300 MHz): δ = 8.53 (s, 1H), 8.14 (s, 2H), 4.99 (m, 1H), 4.41 (s, 2H), 4.41 (q, J = 7.2 Hz, 4H), 1.48 (s, 9H), 1.42 ppm (t, J = 7.2 Hz, 6H); ^{13}C NMR ([D$_6$]DMSO, 50 MHz): δ = 166.7, 155.9, 141.6, 131.9, 131.4, 128.5, 78.1, 42.9, 28.2 ppm; IR (film CsI): $\tilde{\nu}$ = 2980, 2874, 2555, 1709, 1678, 1605, 1519, 1429, 1284, 1166, 945, 890, 758, 694, 481 cm^{-1}; MS (ES): m/z (%): 318 (100) $[M+Na]^+$.

5-(*tert*-Butoxycarbonylaminomethyl)-bis(2,5-dioxopyrrolidin-1-yl)isophthalic ester (20): Compound **19** (250 mg, 0.85 mmol, 1.0 equiv), NHS (254 mg, 0.21 mmol, 2.4 equiv), and DCC (456 mg, 0.21 mmol, 2.4 equiv) were dissolved in anhydrous THF (60 mL) and the reaction mixture was stirred for 12 h at room temperature. The white precipitate was then removed by filtration and the filtrate was evaporated to dryness. The crude was dissolved in ethyl acetate and treated with a saturated aqueous solution of ammonium chloride, dried over $MgSO_4$, filtered, and evaporated to dryness. Purification of the residue by column chromatography on silica gel afforded the desired compound as a white solid (347 mg, 0.71 mmol, 83%). ^{1}H NMR ($CDCl_3$, 200 MHz): δ = 8.76 (s, 1H), 8.34, 8.33 (2s, 2H), 5.23 (m, 1H), 4.43 (m, 2H), 2.91 (s, 8H), 1.44 ppm (s, 9H); ^{13}C NMR ($CDCl_3$, 50 MHz): δ = 169.4, 161.0, 156.2, 142.5, 135.4, 131.5, 127.0, 80.6, 44.1, 28.7, 26.1 ppm; IR (film CsI): $\tilde{\nu}$ = 2979, 2935, 1776, 1742, 1710, 1514, 1367, 1202, 1084, 914, 873, 733, 647 cm^{-1}; MS (ES): m/z (%): 247, 322, 471; unknown fragmentation.

6-(3-{5-Benzyloxycarbonyl-5-[bis(benzyloxycarbonylmethylamino)]}-5-(*tert*-butoxycarbonylaminomethyl)benzoylamino)-2-[bis(benzyloxycarbonylmethylamino)]hexanoic benzyl ester (21): Compound **20** (100 mg, 204 μmol, 1 equiv) was added to a solution of **12** (342 mg, 0.45 mmol, 2.2 equiv) in anhydrous CH_2Cl_2 (13 mL) in the presence of diisopropylethylamine (178 μL, 1.02 mmol, 5 equiv). The reaction mixture was then stirred at room temperature under argon for 12 h, quenched with a saturated aqueous solution of ammonium chloride, dried over $MgSO_4$, filtered, and evaporated to dryness. Purification of the residue by column chromatography on silica gel afforded the desired compound as an oil (223 mg, 0.17 mmol, 82%). ^{1}H NMR ($CDCl_3$, 300 MHz): δ = 8.08 (s, 1H), 7.90 (s, 2H), 7.27 (s large, 30H), 6.84 (m, 2H), 5.06–5.01 (3s, 12H), 4.30 (m, 2H), 3.68 (s, 8H), 3.47 (t, J = 8.4 Hz, 2H), 3.33 (m, 4H), 1.80–1.40 (m, 12H), 1.40 ppm (s, 9H); MS (ES): m/z (%): 1346 (100) $[M+Na]^+$.

6-(3-Aminomethyl-5-{5-benzyloxycarbonyl-5-[bis(benzyloxycarbonylmethylamino)]pentylcarbamoyl}benzoylamino)-2-[bis(benzyloxycarbonylmethylamino)]hexanoic benzyl ester (22): Compound **21** (220 mg, 166 μmol, 1 equiv) was dissolved in CH_2Cl_2 (6 mL) in the presence of trifluoroacetic acid (0.9 mL, 11.6 mmol, 70 equiv). The reaction mixture was stirred at room temperature under an argon atmosphere for 12 h and then concentrated under vacuum. Excess TFA was removed by azeotropic distillation with toluene, thereby affording the desired product as an HCl salt (227 mg, 145 μmol, 86%). ^{1}H NMR ($CDCl_3$, 300 MHz): δ = 8.67 (s large, 2H), 8.18 (s, 1H), 8.13 (s, 2H), 7.77 (s large, 2H), 7.45–7.20 (m, 30H), 5.10, 5.08 (2s, 12H), 4.24 (m, 2H), 3.71 (s, 8H), 3.50 (t, J = 6.9 Hz, 2H), 3.29 (m, 4H), 1.80–1.30 ppm (m, 12H); ^{13}C NMR ($CDCl_3$, 50 MHz): δ = 173.0, 172.1, 167.2, 135.9, 135.5, 134.4, 131.7, 129.0, 128.6, 126.3, 67.1, 66.9, 65.2, 53.5, 50.4, 40.1, 33.8, 30.3, 28.9, 25.8, 23.4 ppm; IR (film CsI): $\tilde{\nu}$ = 3385, 3061, 3033, 2927, 1736, 1677, 1544, 1457, 1199, 1143, 984, 742, 695, 600, 503 cm^{-1}; MS (ES): m/z (%): 1224 (100) $[M+H]^+$, 1246 (2) $[M+Na]^+$.

6-(3-{5-Benzyloxycarbonyl-5-[bis(benzyloxycarbonylmethylamino)]pentylcarbamoyl}-5-[(3-fluoresceinethioureido)methyl]benzoylamino)-2-[bis(benzyloxycarbonylmethylamino)]hexanoic benzyl ester (23): Compound **22** (100 mg, 64 μmol, 1 equiv) was dissolved in anhydrous DMF (1.5 mL) in the presence of *N*,*N*-diisopropylethylamine (DIPEA; 56 μL, 31 μmol, 5.0 equiv). Fluorescein isothiocyanate (FITC; 32 mg, 82 μmol, 1.3 equiv) was then added to the reaction mixture and the resulting solution was stirred at room temperature in the dark overnight. DMF was then removed by means of distillation using a Hickman apparatus and the remaining residue was dissolved in CH_2Cl_2 (15 mL). The organic phase was washed with a saturated aqueous solution of $NaHCO_3$ and with 1% HCl, dried over $MgSO_4$, filtered, and evaporated to dryness. Purification of the residue by column chromatography on silica gel afforded the desired compound as a yellow-orange oil (31 mg, 19 μmol, 30%). ^{1}H NMR ($CD_3OD/CDCl_3$, 300 MHz): δ = 9.19 (s, 1H), 8.86 (s, 1H), 8.68 (m, 3H), 7.77 (m, 31H), 7.70–7.20 (m, 6H), 5.06 (s large, 12H), 5.01 (s, 2H), 3.45 (s, 8H), 3.22 (m, 2H), 3.03 (m, 4H), 1.20–0.70 ppm (m, 12H); ^{13}C NMR ($CD_3OD/CDCl_3$, 50 MHz): δ = 184.4, 175.1, 174.1, 170.5, 166.6, 158.6, 157.4, 148.2, 144.2, 142.1, 138.3, 137.6, 133.6, 131.7, 130.8, 129.7, 127.2, 124.7, 120.7, 120.6, 118.8, 116.1, 104.8, 102.2, 68.7, 67.1, 55.1, 47.0, 42.2, 36.0, 32.2, 30.9, 27.2, 25.5 ppm; IR (film CsI): $\tilde{\nu}$ = 3293, 3035, 2930, 2597, 1740, 1601, 1543, 1456, 1267, 1177, 992, 914, 852, 750, 699, 586, 494, 460, 415 cm^{-1}; HRMS (ES): m/z: calcd for $[M+Na]^+$: 1635.5723; found: 1635.5825.

Compound 7: A 1 M aqueous solution of KOH (335 μL, 335 μmol, 18 equiv) was added to a solution of compound **23** (30 mg, 18.6 μmol, 1.0 equiv) in methanol (1 mL). The reaction mixture was then stirred under argon and in the dark for 18 h at room temperature and then concentrated under vacuum. The residue was dissolved in water (0.5 mL) and the desired product was precipitated by slow addition of a 1 M aqueous solution of HCl. After high-speed centrifugation (13400 rpm) at 0 °C for 15 min, the supernatant was removed and the precipitate was then washed with MeOH and diethyl ether, thereby affording the title compound **7** as a fine orange powder (15 mg, 13.1 μmol, 70%). ^{1}H NMR

($CDCl_3$, 200 MHz): $\delta = 8.35$ (s, 1H), 8.17 (s, 1H), 8.01 (s, 2H), 7.94 (d, $J = 7.6$ Hz, 1H), 7.40–6.70 (m, 7H), 5.00 (s, 2H), 3.78 (s, 8H), 3.67 (m, 2H), 3.43 (m, 4H), 2.00–1.50 ppm (m, 12H); ^{13}C NMR (CD_3OD, 75.5 MHz): $\delta = 183.6$, 175.6, 174.8, 169.5, 166.5, 157.3, 157.2, 143.0, 141.1, 136.6, 132.0, 130.4, 130.1, 129.3, 128.2, 128.0, 126.0, 123.3, 117.1, 103.4, 66.9, 66.4, 55.3, 54.6, 54.5, 54.0, 40.8, 34.7, 30.7, 29.9, 26.0, 24.7 ppm; IR (KBr): $\tilde{\nu} = 3434$, 2928, 2502, 2330, 1964, 1727, 1635, 1548, 1455, 1391, 1314, 1267, 1211, 1116, 854, 795, 701, 445 cm^{-1}; MS (ES): unknown fragmentation.

6-(6-Aminohexanoylamino)-2-[bis(benzyloxycarbonylmethylamino)]hexanoic benzyl ester (27): The corresponding NH-*tert*-butoxycarbonyl (Boc)-protected compound (100 mg, 134 μmol, 1 equiv) was dissolved in anhydrous CH_2Cl_2 (5 mL) containing TFA (725 μL, 9.4 mmol, 70 equiv). The reaction mixture was then stirred under argon for 12 h at room temperature and concentrated under vacuum. Excess TFA was removed by azeotropic distillation with toluene, thereby affording the desired compound as a TFA salt (117 mg, 0.13 mmol, 100%). ^{1}H NMR ($CDCl_3$, 200 MHz): $\delta = 7.59$ (s, large, 2H), 7.40 (brs, 15H), 5.17 (s large, 6H), 3.73 (brs, 4H), 3.58 (t, $J = 6.8$ Hz, 1H), 3.24, 3.08 (2m, 4H), 2.36 (m, 2H), 1.90–1.30 ppm (m, 12H); ^{13}C NMR ($CDCl_3$, 50 MHz): $\delta = 172.7$, 171.7, 135.7, 135.5, 128.7, 128.6, 128.5, 128.3, 77.8, 64.6, 53.2, 39.9, 39.6, 35.3, 29.8, 28.1, 26.6, 25.3, 24.7, 22.9 ppm; MS (ES): *m*/*z* (%): 646 (100) $[M+H]^+$.

6-{6-[3-(5-{5-Benzyloxycarbonyl-5-[bis(benzyloxycarbonylmethylamino)]-pentylcarbamoyl}pentylcarbamoyl)-5-(*tert*-butoxycarbonylaminomethyl)-benzoylamino]hexanoylamino}-2-[bis(benzyloxycarbonylmethylamino]-hexanoic benzyl ester (24): Compound **20** (164 mg, 0.34 mmol, 1.0 equiv) was added to a solution of **27** (645 mg, 738 μmol, 2.2 equiv) in anhydrous CH_2Cl_2 (5 mL) in the presence of diisopropylethylamine (323 μL, 1.85 mmol, 5.5 equiv). The resulting mixture was stirred at room temperature under an argon atmosphere for 12 h, quenched with a saturated aqueous solution of ammonium chloride, dried over $MgSO_4$, filtered, and evaporated to dryness. Purification of the residue by column chromatography on silica gel afforded the desired compound as a white foam (405 mg, 0.26 mmol, 78%). ^{1}H NMR ($CDCl_3$, 300 MHz): $\delta = 8.09$ (s, 1H), 7.85 (s, 2H), 7.27 (m, 30H), 6.11 (m, 2H), 5.37 (m, 1H), 5.02 (s, 12H), 4.28 (m, 2H), 3.64 (s, 8H), 3.40 (m, 6H), 3.07 (m, 4H), 2.10 (m, 4H), 1.80–1.10 ppm (m, 33H); ^{13}C NMR ($CDCl_3$, 100 MHz): $\delta = 173.6$, 172.4, 171.1, 167.0, 135.6, 135.5, 134.9, 129.0, 128.5, 128.0, 127.2, 126.8, 79.5, 66.3, 64.7, 64.4, 52.7, 50.1, 39.8, 39.1, 36.0, 33.7, 29.7, 28.7, 28.3, 26.3, 25.1, 22.9 ppm; IR (CsI film): $\tilde{\nu} = 3045$, 2934, 2862, 1742, 1648, 1543, 1455, 1367, 1259, 1163, 990, 743, 699, 581 cm^{-1}; MS (ES): *m*/*z*: 225, 247, 471, 684; unknown fragmentation.

6-{6-[3-Aminomethyl-5-(5-{5-benzyloxycarbonyl-5-[bis(benzyloxycarbonylmethylamino)]pentylcarbamoyl}pentylcarbamoyl)benzoylamino]hexanoylamino}-2-[bis(benzyloxycarbonylmethylamino)]hexanoic benzyl ester (25): The NH-Boc-protected compound **24** (200 mg, 129 μmol, 1.0 equiv) was dissolved in anhydrous CH_2Cl_2 (5 mL) containing TFA (700 μL, 9.03 mmol, 70 equiv). The reaction mixture was then stirred under argon for 12 h at room temperature and concentrated under vacuum. Excess TFA was removed by azeotropic distillation with toluene, thereby affording the desired compound as a TFA salt (231 mg, 129 μmol, 100%). ^{1}H NMR ($CDCl_3$, 300 MHz): $\delta = 8.58$ (m, 2H), 8.15 (s, 1H), 8.02 (s, 2H), 7.45–7.10 (m, 30H), 7.00 (m, 2H), 5.08 (m, 12H), 4.19 (m, 2H), 3.67 (s, 8H), 3.47 (t, $J = 7.5$ Hz, 2H), 3.34 (m, 4H), 3.13 (m, 4H), 2.24 (m, 4H; H), 1.90–1.10 ppm (m, 24H); ^{13}C NMR ($CDCl_3$, 50 MHz): $\delta = 173.0$, 172.0, 167.4, 136.0, 135.5, 131.6, 131.6, 126.4, 129.0, 128.8, 67.0, 65.1, 53.5, 45.2, 40.5, 39.8, 36.3, 33.7, 30.2, 28.8, 26.6, 25.6, 23.3 ppm; IR (film CsI): $\tilde{\nu} = 3358$, 3036, 2933, 1742, 1646, 1551, 1457, 1202, 992, 802, 747, 700, 598 cm^{-1}; MS (ES): *m*/*z* (%): 1451 (82) $[M+H]^+$.

6-{6-[3-(5-{5-Benzyloxycarbonyl-5-[bis(benzyloxycarbonylmethylamino)]-pentylcarbamoyl}pentylcarbamoyl)-5-[(3-fluoresceinethioureido)methyl]-benzoylamino]hexanoylamino}-2-[bis(benzyloxycarbonylmethylamino)]-hexanoic benzyl ester (26): Compound **25** (278 mg, 155 μmol, 1.0 equiv) was dissolved in anhydrous DMF (4.5 mL) in the presence of diisopropylethylamine (108 μL, 619 μmol, 4.0 equiv). FITC (78 mg, 201 μmol, 1.3 equiv) was then added to the reaction mixture and the resulting solution was stirred at room temperature in the dark overnight. The reaction mixture was then quenched with a 10% aqueous solution of HCl (4 mL) and extracted twice with CH_2Cl_2. The organic phase was dried over $MgSO_4$, filtered, and evaporated to dryness. Purification of the residue by column chromatography on silica gel afforded the desired compound as an orange solid (150 mg, 81.5 μmol, 53%). ^{1}H NMR (CD_3OD, 300 MHz): $\delta = 8.61$ (s, 1H), 8.18 (m, 2H), 8.01 (s, 2H), 7.49 (m, 1H), 7.49 (d, $J = 8.7$ Hz, 2H), 7.11 (d, $J = 8.7$ Hz, 2H), 7.26 (brs, 32H), 5.03 (brs, 12H), 4.96 (s, 2H), 3.70 (s, 8H), 3.50 (t, $J = 7.5$ Hz, 2H), 3.36 (m, 4H), 3.05 (m, 4H), 2.17 (t, $J = 6.9$ Hz, 4H), 1.40–1.20 ppm (m, 24H); ^{13}C NMR ($CDCl_3$, 75.5 MHz): $\delta = 182.9$, 175.8, 173.4, 172.3, 168.8, 167.5, 160.0, 143.4, 140.6, 136.8, 136.1, 133.9, 133.8, 129.4, 129.1, 129.0, 125.9, 120.6, 117.7, 103.3, 67.4, 65.9, 53.7, 40.8, 40.1, 36.8, 30.6, 29.8, 29.5, 27.3, 26.5, 24.0 ppm; IR (KBr): $\tilde{\nu} = 3409$, 2929, 1739, 1633, 1546, 1135, 768, 679, 610 cm^{-1}; MS (ES): *m*/*z*: 1861.7 $[M+Na]^+$, 1883.7 $[M-H+2Na]^+$, 942.7 $[M+2Na]^{2+}$, 953.7 $[M-H+3Na]^{2+}$, 964.6 $[M-2H+4Na)^+$; HRMS (EI): *m*/*z*: calcd for $[M+Na]^+$: 1861.7414; found: 1861.7414; calcd for $[M-H+Na]^+ = 1883.72234$; found: 1883.7116.

Compound 8: A 1M aqueous solution of KOH (294 μL, 294 μmol, 18 equiv) was added to a solution of compound **26** (30 mg, 16.3 μmol, 1.0 equiv) in methanol (1 mL). The reaction mixture was then stirred under argon in the dark for 18 h at room temperature and concentrated under vacuum. The residue was dissolved in water (0.5 mL) and the desired product was precipitated by slow addition of a 1M aqueous solution of HCl. After high-speed centrifugation (13400 rpm) at 0°C for 15 min, the supernatant was removed and the precipitate was then washed with MeOH and diethyl ether to afford the title compound **8** as a fine orange powder (18 mg, 13.9 μmol, 85%). ^{1}H NMR (CD_3OD, 200 MHz): $\delta =$ 8.40–7.90 (m, 4H), 7.50–6.80 (m, 8H), 5.11 (m, 2H), 3.84 (m, 2H), 3.69 (s, 8H), 3.30–3.15 (m, 8H), 2.21 (m, 4H), 1.90–1.20 ppm (m, 24H); ^{13}C NMR (CD_3OD, 50 MHz): $\delta = 183.4$, 176.1, 174.3, 173.6, 169.3, 167.5, 157.7, 143.1, 141.2, 136.6, 132.5, 130.4, 129.6, 129.3, 128.3, 128.0, 125.9, 123.8, 117.7, 103.4, 66.1, 65.2, 54.4, 53.8, 53.4, 52.1, 40.9, 40.1, 37.0, 30.7, 30.1, 29.9, 27.6, 26.7, 24.3 ppm; IR (KBr): $\tilde{\nu} = 3413$, 2927, 1727, 1629, 1548, 1448, 1197, 1172, 1119, 801, 690, 439 cm^{-1}; MS (ES): unknown fragmentation.

H_6SRC1 expression and purification: The PQE_{30}-$SRC1_{570-580}$ plasmid required for the $SRC1_{570-580}$ expression was kindly provided by C. Royer (CBS, Montpellier, France). The H_6-tagged $H_6SRC1_{570-580}$ protein (designated by H_6SRC1) was over-expressed in *Escherichia coli* and purified by Ni^{2+}–NTA agarose beads under native conditions (Qiagen, Courtaboeuf, France).

Direct-binding assay: Binding assays were performed using a Beacon 2000 polarization instrument (Panvera, Madison, WI, USA) regulated at 20°C, using filters for fluorescein at an H_6SRC1 concentration of 30 μM. All solutions were freshly prepared using the buffer solution **P** (10 mM Tris, 150 mM NaCl, 10% glycerol, pH 8.0). Buffer **P** (50 μL), 90 μM H_6SRC1 (50 μL), and 30 nM Ni^{2+}–NTA–fluorescein (50 μL; or 50 μL of 60 nM Ni_2–**7** or Ni_2–**8**) were successively added in a borosilicate tube. Each point in the titration curve was then obtained by removing aliquots of 100 μL from the starter solution and replacing them by 100 μL of 15 nM Ni^{2+}–**1** probe (or 100 μL of 30 mM Ni_2–**7** or Ni_2–**8**). Tubes were equilibrated at 20°C for 4 min prior to measurement and the polarization was measured successively until stabilized. The reported values are the average of three measurements after stabilization.

In parallel, additional experiments were performed under the same conditions but in the absence of nickel. The obtained values were then subtracted from the previous ones to give the specific polarization values.

Competition binding assays (displacement curve of Ni^{2+}–1 by bis-NTA–$(Ni^{2+})_2$ ligands): The polarization measurements have been carried out using an AD Analyst apparatus (Molecular Devices, Sunnyvale, USA) equipped with a dichroic filter (485 nm/530 nm) using Dynex Microfluor 96 polystyrene well plates (8 rows and 12 columns). Polarization values were obtained by reading the microplates at 20°C at half-height of the wells. All solutions were freshly prepared using the buffer solution **P** (10 mM Tris, 150 mM NaCl, 10% glycerol, pH 8.0). Each well of the plate was preincubated with a 30 μM solution of H_6SRC1 (50 μL) and a 5 nM solution of Ni–**1** (50 μL). After a 20 min period of incubation at room temperature, each well of the first column was then rapidly treated with

additional buffer solution (50 μL) containing decreasing concentrations of NTA–Ni (1 mM; 100, 30, 10, 1, 0.1, and 0.01 μM). Using the same procedure, columns 2, 3, 4, 5, and 6 were successively treated respectively with bis-NTA **2**, **3**, **4**, **5**, and **6** previously incubated for 2 h at 5°C with two equivalents of nickel. The plate was read immediately after this treatment to provide raw polarization values.

The plotted specific polarization values were obtained by subtracting from the raw polarization values the nonspecific polarization value. The latter can be obtained by mixing, in one well, a 30 μM solution of H_6SRC1 (50 μL), the buffer solution **P** (50 μL), and a 5 nM solution of NTA–fluorescein (50 μL). Additionally, the total binding can be obtained by mixing, in one well, a 30 μM solution of H_6SRC1 (50 μL), the buffer solution **P** (50 μL), and a 5 nM solution of Ni–**1** (50 μL).

Isothermal titration calorimetry (ITC) experiments: Calorimetry was a convenient thermodynamic approach to monitor any chemical reaction initiated by the addition of binding components. By measuring the heat generated or absorbed during the association between interacting species, this method allows full determination of multiple thermodynamic parameters, such as the binding constants (K_D), the reaction stoichiometry (n), the binding enthalpy (ΔH), and the entropy (ΔS) as well. All binding experiments were performed using an isothermal titration calorimeter from Microcal Inc (Northampton, MA, USA). All solution of injected (**I**) and titrated (**T**) species in buffer **A** (100 mM Tris, 150 mM NaCl, pH 8.0) were freshly prepared and thoroughly degassed for 15 min at 17°C prior to measurement. An equilibration period of 30–45 min was used before starting the experiment.

In a typical experiment, the calorimetric cell was filled with a **T** solution (1.419 mL) of concentration C_T (pH 8.0) and fifty-eight consecutive additions of 5 μL of a **I** solution of concentration C_I (pH 8.0) for a total volume of 290 μL added guest. The first ten injections were performed with an interval of 5 min to ensure that the titration peak returned to the baseline prior to the next injection. The next 48 injections were conducted with a shorter interval period of 3 min. The temperature (20°C) remained constant during the entire experiment and continuous stirring was required to ensure rapid mixing of the reaction mixture. Dilution effects were measured in a separate experiment by adding the same **I** solution into pure buffer **A** and subtracted from the previous experiment. The resulting binding data were processed with the Origin software to obtain the thermodynamic parameters of the interaction.[30] All the concentration values and the regression models used for each assay are given in the Supporting Information.

Acknowledgements

This work was supported by the CNRS, the University of Strasbourg, and Astra-Zeneca. Dr. J.-C. Bonnafous from INSERM is acknowledged for fruitful scientific discussions and collaboration. We thank Dr. C. Royer from CBS, Montpellier, for offering the plasmid material needed for the protein H_6SRC1 expression. We are grateful to P. Vassault and A. Bourdoncle for help with protein expression, and to Dr. C. Maechling from the University of Strasbourg for scientific discussion on ITC.

[1] B. A. Griffin, S. R. Adams, R. Y. Tsien, *Science* **1998**, *281*, 269.
[2] S. R. Adams, R. E. Campbell, L. A. Gross, B. R. Martin, G. K. Walkup, Y. Yao, J. Llopis, R. Y. Tsien, *J. Am. Chem. Soc.* **2002**, *124*, 6063–6076.
[3] Z. Zhang, B. A. Smith, L. Wang, A. Brock, C. Cho, P. G. Schultz, *Biochemistry* **2003**, *42*, 6735–6746.
[4] A. Keppler, S. Gendreizig, T. Gronemeyer, H. Pick, H. Vogel, K. Johnsson, *Nat. Biotechnol.* **2003**, *21*, 86–89.
[5] J. Yin, F. Liu, X. Li, C. T. Walsh, *J. Am. Chem. Soc.* **2004**, *126*, 7754–7755.
[6] R. J. Wood, D. D. Pascoe, Z. K. Brown, E. M. Medlicott, M. Kriek, C. Neylon, P. L. Roach, *Bioconjugate Chem.* **2004**, *15*, 366–372.
[7] N. George, H. Pick, H. Vogel, N. Johnsson, K. Johnsson, *J. Am. Chem. Soc.* **2004**, *126*, 8896–8897.
[8] I. Chen, M. Howarth, W. Lin, A. Y. Ting, *Nat. Methods* **2005**, *2*, 99–104.
[9] I. Chen, A. Y. Ting, *Curr. Opin. Biotechnol.* **2005**, *16*, 35–40.
[10] K. Terpe, *Appl. Microbiol. Biotechnol.* **2003**, *60*, 523–533.
[11] a) M. Popp, J. M. Antos, G. M. Grotenbreg, E. Spooner, H. L. Ploegh, *Nat. Chem. Biol.* **2007**, *3*, 1–2; b) H. M. O'Hare, K. Johnsson, A. Gautier, *Curr. Opin. Struct. Biol.* **2007**, *17*, 488–494; c) E. G. Guignet, J.-M. Segura, R. Hovius, H. Vogel, *ChemPhysChem* **2007**, *8*, 1221–1227; d) A. Gautier, A. Juillerat, C. Heinis, I. R. Corrêa, M. Kindermann, F. Beaufils, K. Johnsson, *Chem. Biol.* **2008**, *15*, 128–136; e) c. T. Hauser, R. T. Tsien, *Proc. Natl. Acad. Sci. USA* **2007**, *104*, 3693–3697.
[12] M. S. T. Gonçalves, *Chem. Rev.* **2009**, *109*, 190–212.
[13] a) E. Hochuli, H. Dobeli, A. Schacher, *J. Chromatogr.* **1987**, *411*, 177–184; b) E. K. Ueda, P. W. Gout, L. Morganti, *J. Chromatogr. A* **2003**, *988*, 1–23.
[14] C. Hart, B. Schulenberg, Z. Diwu, W. Y. Leung, W. F. Patton, *Electrophoresis* **2003**, *24*, 599–610.
[15] a) J. Kim, H.-Y. Park, J. Kim, J. Ryu, Kwon, Y. Do, R. Grailhe, R. Song, *Chem. Commun.* **2008**, 1910–1912; b) W. Shen, H. Zong, D. Neff, M. Norton, *J. Am. Chem. Soc.* **2009**, *131*, 6660–6661.
[16] a) P. D. Gershon, S. Khilko, *J. Immunol. Methods* **1995**, *183*, 65–76; b) E. L. Schmid, T. A. Keller, Z. Dienes, H. Vogel, *Anal. Chem.* **1997**, *69*, 1979–1985; c) C. Xu, K. Xu, H. Gu, X. Zhong, Z. Guo, R. Zheng, X. Zhand, B. Xu, *J. Am. Chem. Soc.* **2004**, *126*, 3392–33–93; d) L. Schmitt, M. Ludwig, H. E. Gaub, R. Tampé, *Biophys. J.* **2000**, *78*, 3275–3285.
[17] a) L. Schmitt, C. Dietrich, R. Tampé, *J. Am. Chem. Soc.* **1994**, *116*, 8485–8491; b) C. Dietrich, L. Schmitt, R. Tampé, *Proc. Natl. Acad. Sci. USA* **1995**, *92*, 9014–9018; c) I. T. Dorn, R. Eschrich, E. Seemuller, R. Guckkenberger, R. Tampé, *J. Mol. Biol.* **1999**, *288*, 1027–1036.
[18] a) G. B. Sigal, C. Bamdad, A. Barberis, J. Strominger, G. M. Whitesides, *Anal. Chem.* **1996**, *68*, 490–497; b) L. Nieba, S. E. Nieba-Axmann, A. Persson, M. Hamalainen, F. Edebratt, A. Hansson, J. Lidholm, K. Magnusson, A. F. Karlsson, A. Pluckthun, *Anal. Biochem.* **1997**, *252*, 217–228; c) I. T. Dorn, K. Pawlitschko, S. C. Pettinger, R. Tampe, *Biol. Chem.* **1998**, *379*, 1151–1159.
[19] a) I. T. Dorn, K. R. Neumaier, R. Tampé, *J. Am. Chem. Soc.* **1998**, *120*, 2753–2763; b) A. Tinazli, J. Tang, R. Valiokas, S. Picuric, S. Lata, J. Piehler, B. Liedberg, R. Tampé, *Chem. Eur. J.* **2005**, *11*, 5249–5259.
[20] A. N. Kapanidis, Y. W. Ebright, R. H. Ebright, *J. Am. Chem. Soc.* **2001**, *123*, 12123–12125.
[21] S. Hutschenreiter, L. Neumann, U. Radler, L. Schmitt, R. Tampé, *ChemBioChem* **2003**, *4*, 1340–1344.
[22] a) I. T. Dorn, K. Pawlitschko, S. C. Pettinger, R. Tampé, *Biol. Chem.* **1998**, *379*, 1151–1159; b) R. D. Johnsson, R. J. Todd, F. H. Arnold, *J. Chromatogr. A* **1996**, *725*, 225–235; c) S. Lata, J. Piehler, *J. Anal. Chem.* **2005**, *119*, 1096–1105.
[23] S. Lata, A. Reichel, R. Brock, R. Tampé, J. Piehler, *J. Am. Chem. Soc.* **2005**, *127*, 10205–10215.
[24] S. Lata, M. Gavutis, R. Tampé, J. Piehler, *J. Am. Chem. Soc.* **2006**, *128*, 2365–2372.
[25] E. G. Guignet, R. Hovius, H. Vogel, *Nat. Biotechnol.* **2004**, *22*, 440–444.
[26] Y. Zhang, S. Akilesh, D. Wilcox, *Inorg. Chem.* **2002**, *41*, 3057–3064.
[27] C. R. Goldsmith, J. Jaworski, M. Sheng, S. J. Lippard, *J. Am. Chem. Soc.* **2006**, *128*, 418–419.
[28] R. O'Brien, J. E. Ladbury, B. Z. Chowdhry, *Biocalorimetry Applications of Calorimetry in the Biologial Sciences*, Wiley, New York, **1998**.
[29] ITC data were recorded and analyzed with VP Viewer and Origin softwares furnished by Microcal Inc (Northampton, MA, USA).
[30] D. Tareste, F. Pincet, M. Brellier, C. Mioskowski, E. Perez, *J. Am. Chem. Soc.* **2005**, *127*, 3825–3829.

[31] K. A. Connors, *Binding Constants—The Measurements of Molecular Complex Stability*, Wiley, New York, **1987**.
[32] M. Rekharsky, Y. Inoue, S. Tobey, A. Metzger, E. Anslyn, *J. Am. Chem. Soc.* **2002**, *124*, 14959–14967.
[33] T. Stora, R. Hovius, Z. Dienes, M. Pachoud, H. Vogel, *Langmuir* **1997**, *13*, 5211–5213.
[34] C. Seel, A. H. Parham, O. Safarowsky, G. M. Huebner, F. Voegtle, *J. Org. Chem.* **1999**, *64*, 7236–7242.
[35] S. M. Dimick, S. C. Powell, S. A. McMahon, D. N. Moothoo, J. H. Naismith, E. J. Toone, *J. Am. Chem. Soc.* **1999**, *121*, 10286.

Received: May 7, 2009
Published online: October 28, 2009

